

EFFECT OF SOLAR HEATING OVER THE PROPELLANT TEMPERATURE IN A SOLID ROCKET ENGINE

Carlos Lavrado Filho

Humberto Araujo Machado, humbertoam@iae.cta.br

Instituto de Aeronáutica e Espaço – IAE

Comando-Geral de Tecnologia Aeroespacial – CTA

Pr. Mal. Eduardo Gomes, 50, Vila das Acácias

12228-904

São José dos Campos, SP

Abstract. During the integration phase and pre-launching period, a space vehicle may suffer a long exposition to solar radiation in the launching pad. Due the heat transfer through engine walls, the propellant temperature rises, what can affect its chemical and mechanical properties, and cause undesirable deformation over its internal profile. In this work, the solid propellant heating of the VLS first stage is estimated via a transient computational simulation, in order to determine if the reached temperature are under the limits of operation.

Keywords: Solid propellant, Multi-layer heat conduction, Solar heating.

1. INTRODUCTION

One of the most critical phases of a space vehicle launching is the pre-launching, when all the components (engines and payload) are mounted and integrated and the vehicle is put on the launch pad. This activity is commonly done in a protected environment, frequently with controlled temperature and humidity. After integration, the vehicle remains exposed to the external environment, standing by the launching (Palmério, 2004).

The integration of VLS (Satellite Launcher Vehicle) developed by IAE-CTA is done within the TMI (*Mobile Integration Tower*), straight over the launch pad (which is kept inside the tower during the integration), available at the CLA (*Alcântara Launching Center*). After mounting, the TMI is brought away, allowing VLS launching, Fig. 1.

Since the VLS is exposed, there are still several activities to be completed before launching, like the evaluation of atmosphere conditions (wind and precipitation), for example. If such conditions are not considered adequate, the launching is postponed, that may keep the vehicle exposed to the daylight for some hours.

In this case, the incidence of solar radiation over the vehicle surface yields a heating that propagates to its interior, which has to be taken into account over all its components. A specific problem is to guarantee that the temperature of the solid propellant do not overpass the maximum value specified (60°C). Above such temperature, some undesirable effects will occur: deformation of propellant profile inside the engine, loosing of mechanical characteristics, appearing of grooves and modification of physical and chemical properties, that could cause malfunctioning of the engines, and eventually result in the lost of vehicle.

In this work, the maximum temperature reached by the propellant of 1st stage engines of VLS is estimated, assuming a complete daily exposure to solar radiation. The calculation is done through numerical simulation, considering the geometry and physical properties of materials employed in all solid fuel layers. Results indicate that the final temperature reached is below the limit, allowing a safety launching concerned to this aspect.



Figure 1. Sequence of integration and releasing of VLS from TMI, before launching.

2. PHYSICAL PROBLEM

VLS configuration is showed in Fig. 2. The first stage consists of four solid propellant boosters, disposed symmetrically around the central stage. The vehicle stays at vertical position after integration. Constructive details are showed in Fig. 3. Although the engine presents a cylindrical external shape, the internal surface of propellant has star-shaped section, and it means that internal diameter varies from the base to top. Since the nozzle (at the bottom) and the top are smaller than the engine diameter, and it has no contact with the propellant, the heat conduction from those regions can be neglected. As the nozzle is opened, the empty space inside the propellant is filled with atmospheric air. This internal air is considered static and thermally insulated from the environment (against convection and radiation), which allows considering the internal surface of the propellant as thermally insulated.

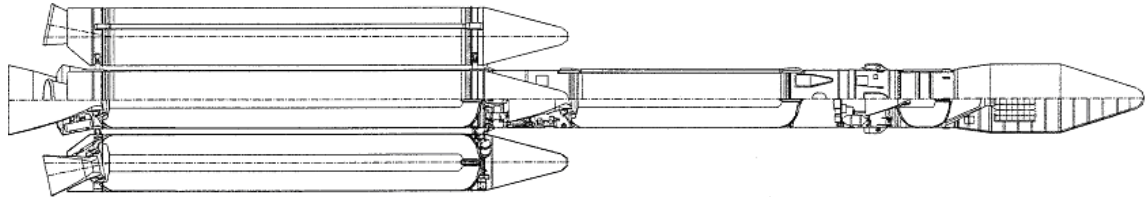


Figure 2. VLS configuration.



Figure 3. View of a booster of VLS's 1st stage.

3. MATHEMATICAL MODELLING

The following hypothesis were considered:

- Constant properties in every material.
- Internal surface thermally insulated.
- Natural convection over the external surface (absence of wind, which is the more critical condition).
- Radiation absorbed in solar band and emitted in infrared band.

The heat transfer within the engine layers is represented by the two-dimension unsteady heat conduction equation, in cylindrical coordinates.

$$\frac{\partial T}{\partial t} = \alpha \left[\frac{1}{r} \frac{\partial}{\partial r} \left(r \frac{\partial T}{\partial r} \right) + \frac{\partial^2 T}{\partial z^2} \right] \quad (1)$$

where α is the thermal diffusivity, and T, t, r and z corresponds to temperature, time, radial and axial coordinates, respectively. One should note that the equation is to be solved separately but simultaneously for all layers, through the coupling boundary condition:

$$-k_i \frac{\partial T_i}{\partial r} \Big|_{r=r_i} = -k_{i+1} \frac{\partial T_{i+1}}{\partial r} \Big|_{r=r_i} \quad (2)$$

where k is the thermal conductivity, the subscript i refers to a specific layer and r_i is the radial coordinate of its external boundary. The boundary condition for the internal surface of the first layer (propellant) will be:

$$-k \frac{\partial T}{\partial r} \Big|_{r=r_{i0}} = 0 \tag{3}$$

where r_{i0} is the propellant's local internal radius. The boundary condition for the external surface of the last layer (painted steel wall), obtained after an energy balance, is:

$$-k \frac{\partial T}{\partial r} \Big|_{r=r_w} = (1 + \eta) \cdot \alpha_{ss} \cdot \dot{q}_s - \sigma \cdot \varepsilon_{is} (T_w - T_{\infty}) - h \cdot (T_w - T_{\infty}) \tag{4}$$

where r_w is the engine external radius, η is the albedo, α_{ss} is the absorvity for solar band of the external surface, σ is the Stefan-Boltzman constant, ε_{is} is the emissivity in the infrared band, q_s is the solar radiative heat flux, T_w and T_{∞} are respectively the temperatures of the external wall and environment, and h is the convective heat transfer coefficient. The first term is heat flux crossing the external surface. In the right hand-side, the first term is the solar radiation absorbed by the external surface, that corresponds to the direct incident solar radiation plus the fraction scattered by the environment; second term is the radiation emitted by the surface. Due its low temperature, most of the emission will be in the infrared band. The last term corresponds to the heat lost to the air by convection. Values used for calculation are showed in Tab.1. Those values were obtained from experimental measurements (Garcia, 1996), except h , that was extracted from literature (Kreith & Bohn, 2003), considering the lower value (natural convection). The term q_s is a time-dependent function, its curve was obtained from measurements at *CLA*, between 1998 and 2000, and it is showed in Fig. 4. Physical properties for the materials use in each layer are showed in Tab. 2.

Table 1. Values assumed for constants in Eq. (4).

Symbol	Description	Experimental value
ε_{is}	Emissivity in the infrared band	0,898
α_{ss}	Absorvity in the solar band	0,164
T_{∞}	Atmospheric air temperature	300 K
h	Convection heat transfer coefficient	6,0 W/m ² K
η	Albedo	0,3

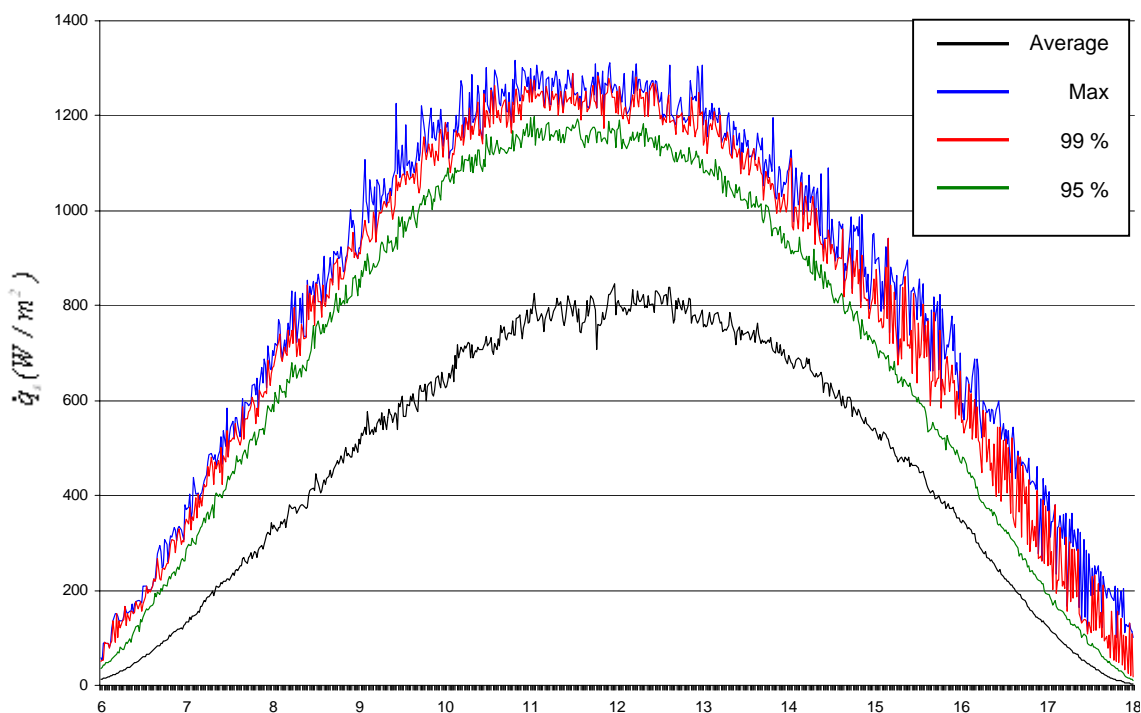


Figure 4. Incident solar radiation during the day in Alcântara (Fish, 2005).

Table 2. Physical properties for the materials used in each layer (Timóteo, 2006).

	1 st layer (internal)	2 nd layer	3 rd layer	4 th layer (external)
Material	Propellant	Liner	Rubber	Stainless Steel ⁽¹⁾
k (W/m.K)	0.17	0.09	0.31	18
C_p (J/kg.k)	1200	1670	1480	460
ρ (kg/m³)	1710	980	1300	7800
α (m²/s)	8.28 x 10 ⁻⁸	4.68 x 10 ⁻⁸	1.89 x 10 ⁻⁷	5.01 x 10 ⁻⁶
Thickness	Variable	3 mm	2-10 mm	3.3 mm

(1) Extracted from COSMOS databank (Dassault Systemes S.A., 2004).

4. SOLUTION

Equation (1), with the boundary conditions, Eqs. (2-4), was solved via the Finite Element Method, through the software COSMOS (Dassault Systemes S.A., 2004), available at the Space-Systems Division (ASE) of IAE-CTA. The computational grid was constructed from a CAD model, showed in Fig 5. In that figure, it is remarkable that the diameter and dimensions of the internal star profile of the solid fuel varies along the length. The transversal section obtained from the A-A cut in Fig. 5. Taking advantage of the partial symmetry of the engine, only a fraction of the domain has to be analyzed. Figure 6.a shows a two-dimensional grid in a transversal section of the motor, which was considerably reduced through that strategy. Figure 6.b shows a grid detail, were a specific grid for each layer can be observed.

The unstructured grid effectively used for the solution is showed in Fig. 7. In that figure, it is evident that the “star profile” does not follow the propellant extension, and neglecting such geometry variation could cause some loss of accuracy. The program was validated comparing the steady value of the wall temperature, obtained from the solution of the unsteady problem, with the result for steady state, considering a fixed value for solar constant (1400 W/m²) and neglecting the convection effects. In both cases, the result was the same (533° C).

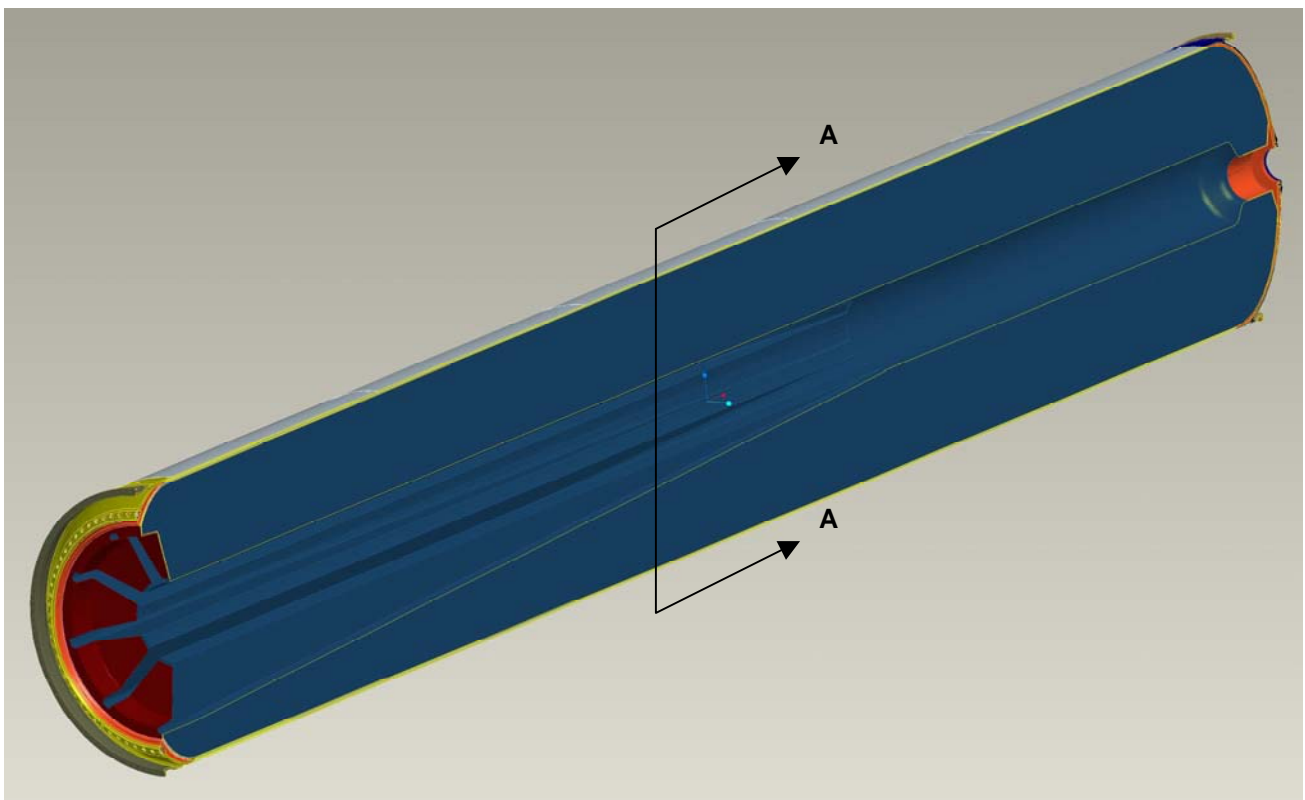
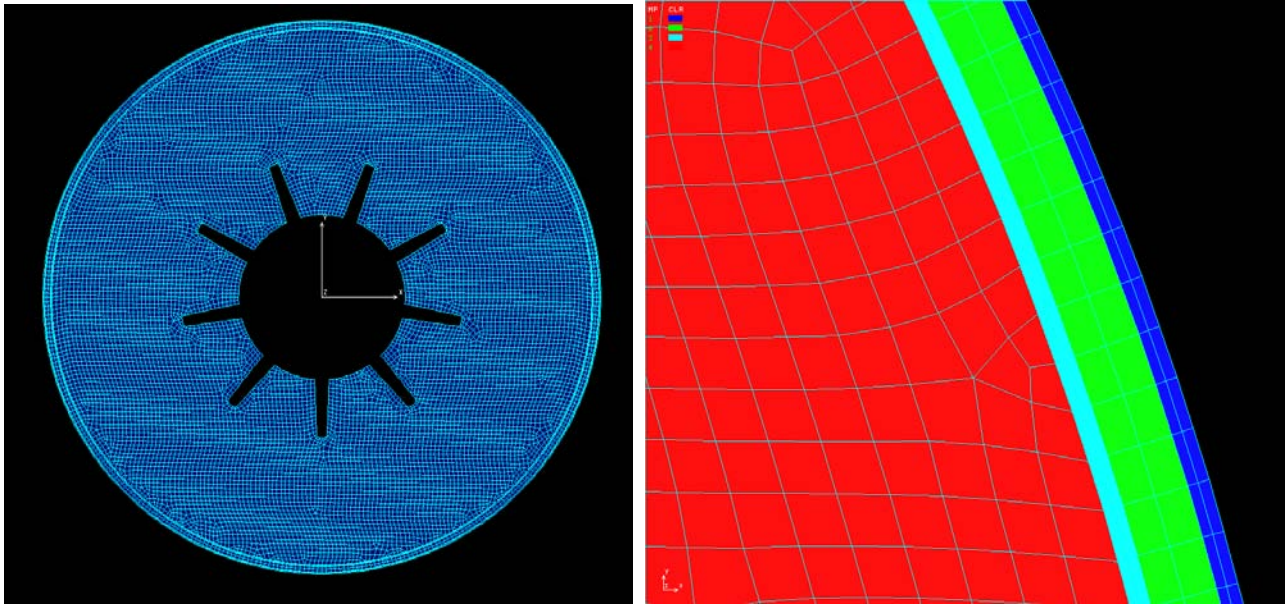


Figure 5. Detail of a booster.



(a) Transversal section A-A

(b) Grid detail with layers

Figure 6. Transversal section with grid.

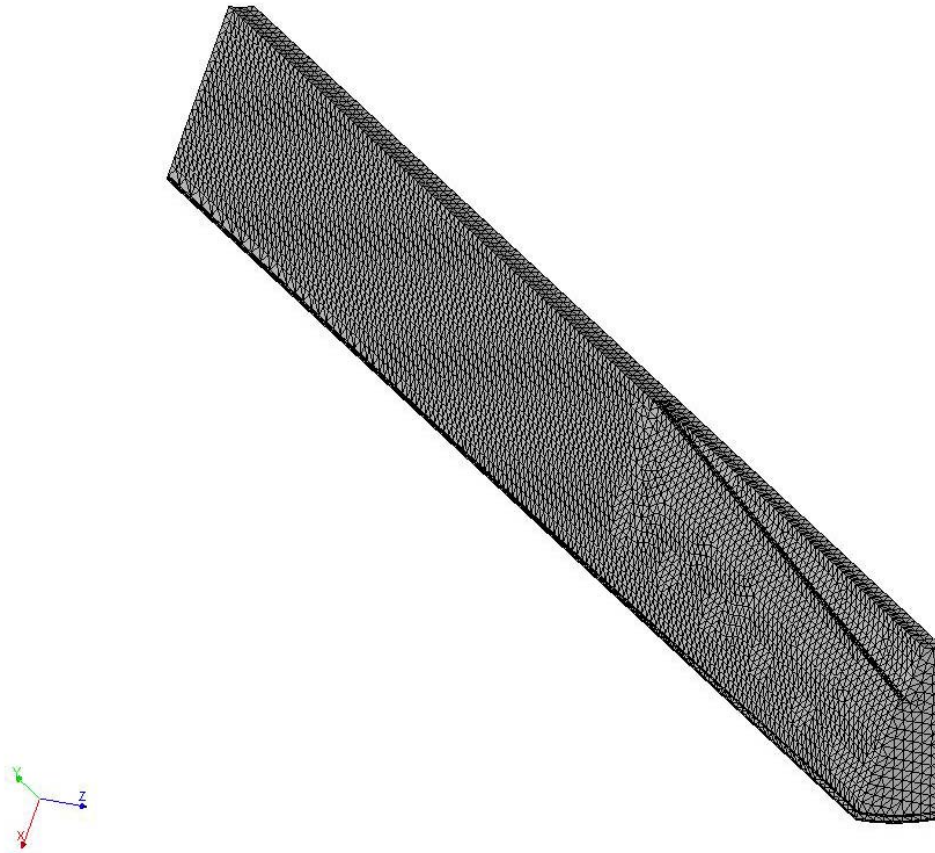


Figure 7. Three-dimensional grid over domain, select for solution.

5. RESULTS

Results for the complete transient simulation are shown in Figs. 8-12. In Fig. 8, the temperature variation during the daily period indicates that the maximum value for the external wall temperature is reached after 6 hours of exposition. The external wall reaches 318 K (45° C) and then begins to fall, due the solar radiation decreasing.

Propellant temperature presents a delay, due the thermal insulation caused by the presence of the rubber and liner layers, and its peak is reached two hours latter. The maximum value found in the external boundary of propellant layer is 312° C, considerable lower then the upper limit (60° C), and falling to about 35° C at the end of the daylight period.

It should be noted that this peak do not correspond to the average temperature of the propellant bulk temperature. Figures 9-12 shows that only the thin region close to the interface presents such values. Most of the propellant keeps at the initial temperature (300 K, or 27° C), since the material is a good thermal insulator, what combines to its high thermal inertia to reduce the temperature variation. A consequence of this behavior is that, at the end of the heating period, the maximum propellant temperature overpasses the external wall temperature, as shown in Fig. 8.

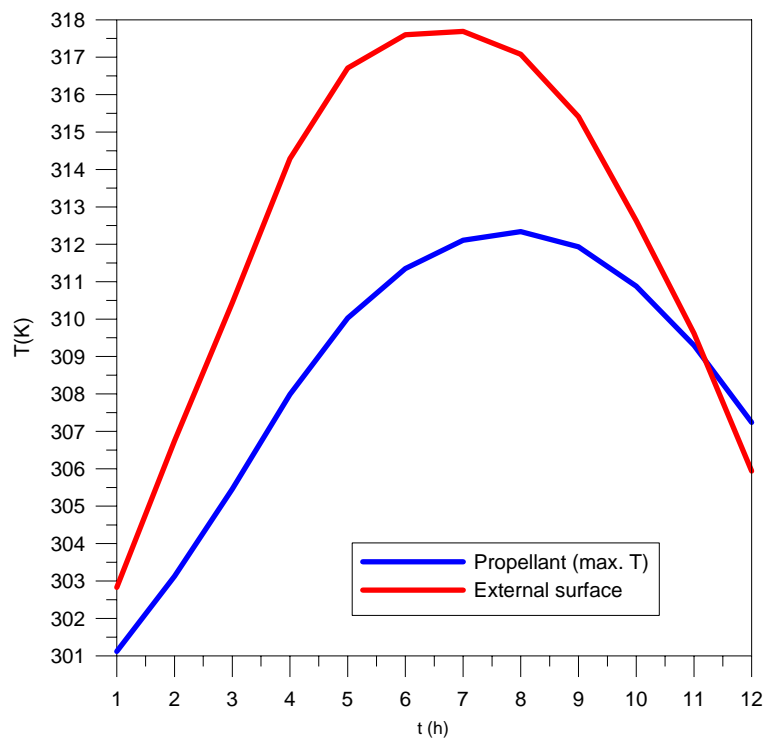


Figure 8. Temperature variation for propellant (external edge) and wall (external surface).

6. CONCLUSION

In this work, the maximum temperature reached by the propellant of the solid rocket engine of the VLS 1st stage, after a long exposure to solar radiation was estimated via numerical simulation, in order to determine if the upper temperature limit was over passed. The software package COSMOS was used to solve the three-dimensional unsteady heat conduction problem in a multi-layer cylindrical domain, employing a unstructured grid generated from a CAD model, and considering the thermal properties experimental evaluation done in IAE-CTA. Since the value found (38° C) is quite lower than the limit, the pre-launching condition is considered safety concerned to this particular aspect.

7. ACKNOWLEDGEMENTS

The authors would like to acknowledge the financial support provided by CNPq during the development of this work.

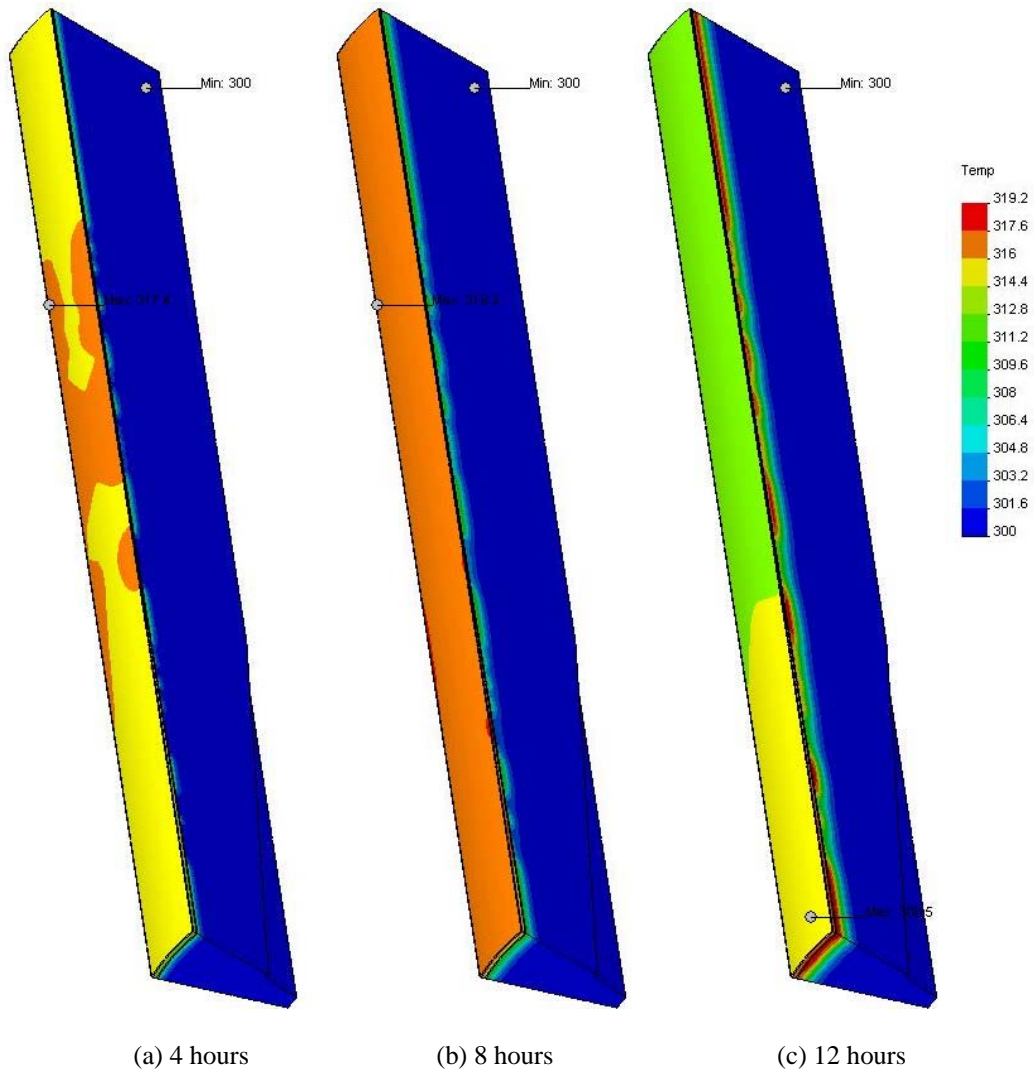


Figure 9. Temperature profiles of domain according to the time of exposition.

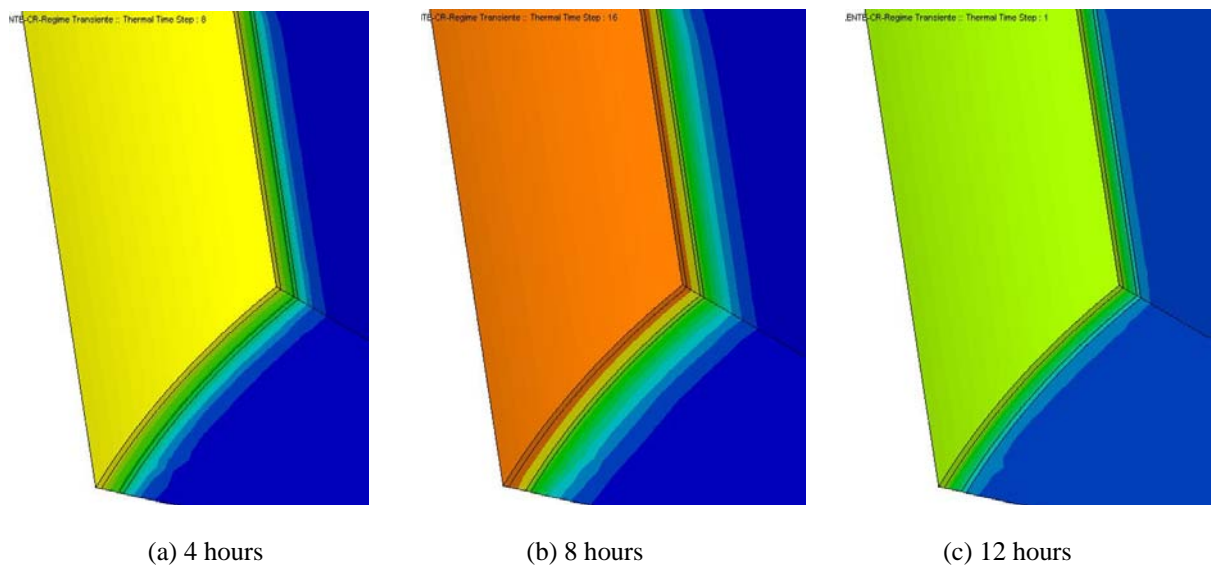


Figure 10. Temperature profiles of domain – detail of layers.

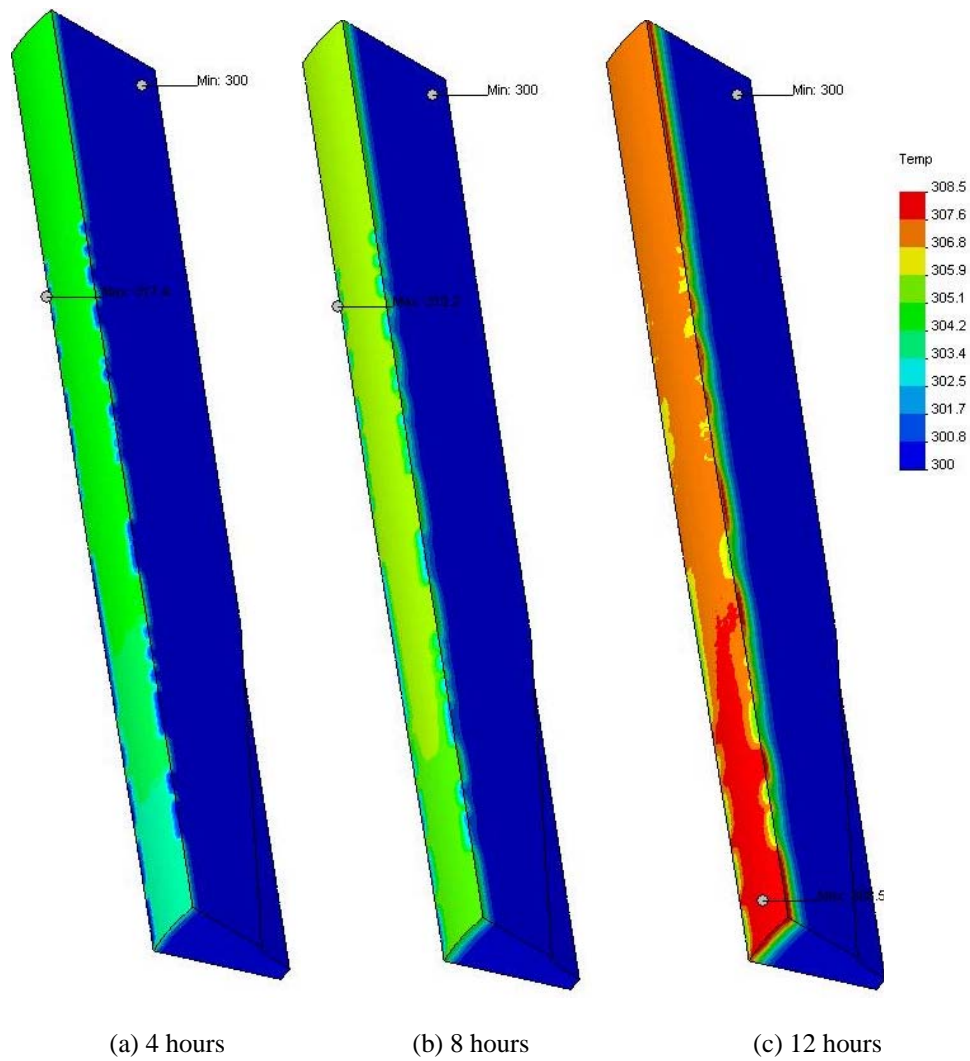


Figure 11. Temperature profiles of propellant according to the time of exposition.

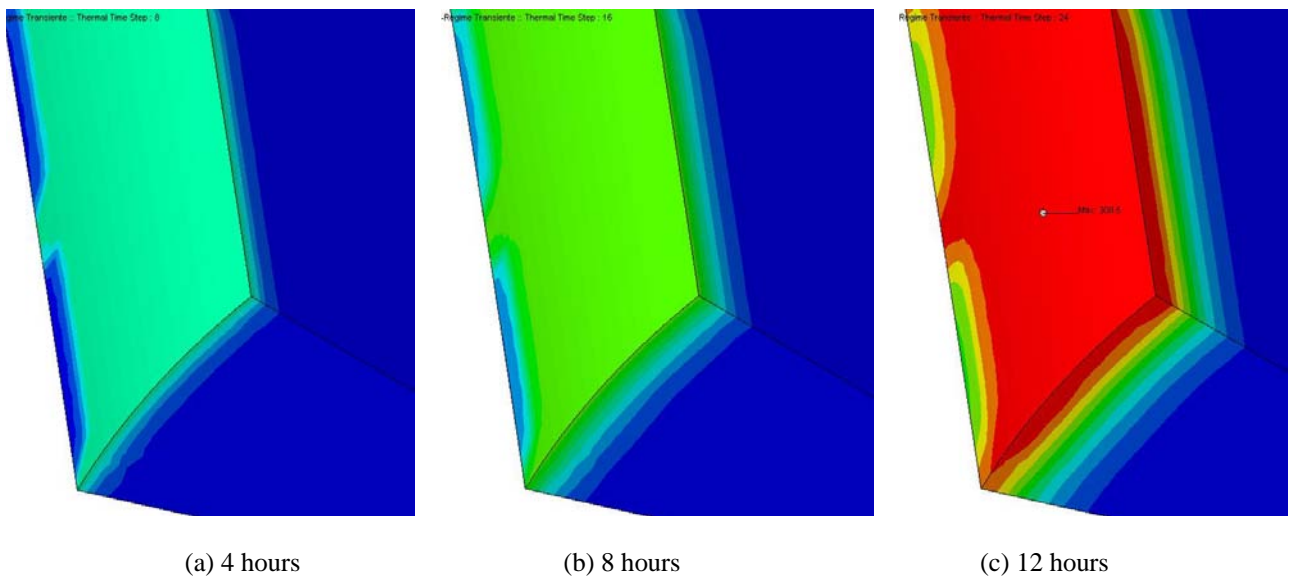


Figure 12. Temperature profiles of domain – detail of external surface.

8. REFERENCES

- Dassault Systemes S.A., 2004, “Cosmos User’s Guide”.
- Fisch, G., 2005, “Incidência de Radiação Solar no CLA”, Internal Communication, IAE/CTA, São José dos Campos.
- Garcia, E. C., 1996, “Medidas de Propriedades Termo-Ópticas”, Doc. INPE/LIT.PG 004/96, São José dos Campos.
- Kreith, F., Bohn, M. S., 2003, “Princípios de Transferência de Calor”, Thomson, São Paulo.
- Palmério, A. F., 2004, “Introdução à Tecnologia de Foguetes”, IAE/CTA, São José dos Campos.
- Thimoteo, H. P. de C. A., 2006, “Propriedades do Materiais do Motor a Propelente Sólido – VLS”, Internal Communication, IAE-CTA, São José dos Campos

9. RESPONSIBILITY NOTICE

The authors are the only responsible for the printed material included in this paper.